

Methods and application of using detrital zircons to trace the provenance of loess

XIE Jing^{*}, YANG ShiLing & DING ZhongLi

*Key Laboratory of Cenozoic Geology and Environment, Institute of Geology and Geophysics,
Chinese Academy of Sciences, Beijing 100029, China*

Received November 30, 2011; accepted March 12, 2012; published online May 23, 2012

The composition of single-grain detrital zircons is an effective provenance indicator of loess, and sheds new light on dust formation and transportation. Here we review the features of detrital zircons and their use as a provenance indicator, including internal structure, trace element, U-Pb age spectrum and Hf isotopic compositions, and present a case study from the Horqin sandy land and its surrounding loess. The loess samples have detrital zircon age peaks in range of 2600–2300, 2100–1600, and 600–100 Ma, of which the 2600–2300 Ma zircon grains mainly have positive $\varepsilon_{\text{Hf}}(t)$ values (–3.4–8.7), the 2100–1600 Ma zircon grains mainly have negative $\varepsilon_{\text{Hf}}(t)$ values (–10.1–6.8), and the 600–100 Ma zircon grains have a variable $\varepsilon_{\text{Hf}}(t)$ values ranging from –21 to 15.9. The detrital zircon signatures of the loess are similar to the Horqin sandy land, but clearly different from the Chinese Loess Plateau and central-western deserts, implying that the loess is transported mainly from the Horqin sandy land in the Last Glacial period. Comparing these with neighboring tectonic units, we found that zircon populations at 2600–2300, 2100–1600, and 600–100 Ma with negative $\varepsilon_{\text{Hf}}(t)$ values may come from the northeast North China Craton (NCC), and those at 600–100 Ma with positive $\varepsilon_{\text{Hf}}(t)$ values may come from the east Central Asian Orogenic Belt (CAOB). It is estimated that the two sources contribute equally to the Horqin sandy land and the surrounding loess.

loess provenance, detrital zircon, U-Pb age, Hf isotope, Horqin sandy land

Citation: Xie J, Yang S L, Ding Z L. Methods and application of using detrital zircons to trace the provenance of loess. *Sci China Earth Sci*, 2012, 55: 1837–1846, doi: 10.1007/s11430-012-4428-x

As eolian deposits, before final accumulation, loess experienced a series of processes in arid area including production of fine-particle material, sorting, mixture and transportation. Understanding these processes is important to reconstruct surface processes of arid area and atmospheric circulation patterns. To date, the consensus in academic community is that loess of the Chinese Loess Plateau was produced in mountains and plateau of western China, and then was transported to the Chinese Loess Plateau or farther regions by winds in desert environments. But it is a kind of simple and sketchy characterization. Some problems such as rela-

tive contributions of different sources and transportation pathways cannot be solved because of the lack of effective means. For example, many researchers apply geochemistry (such as element, Nd, Sr, Pb, Hf, Os isotope) [1–7], mineralogy (such as O isotope, crystallinity and ESR signal intensity of quartz, dolomite content) [8–10], and sedimentology methods (such as sedimentation rate, grain size sorting) [11–14]. The mixed samples are measured by geochemical and traditional mineralogical methods. Although the initial source region can be pointed out sometimes, these methods are incapable of determining contributions of different sources. Loess is a mixture of many source areas, even its chemical composition is considered as the average of upper crust [15–18]. If geochemical characteristics of

*Corresponding author (email: xiejing@mail.igcas.ac.cn)

loess lie between several potential source areas, it originates from single source or a mixture of two or multiple sources. In addition, these methods are incapable of tracing the process that dust grains are transported from erosion area to deposition area. Sedimentology methods only indicate the last-station source before deposited in the Loess Plateau, and cannot demonstrate the initial source areas. Because these tracing methods have their own limitations, sources of dust are too complicated to sort out. Different conclusions can be made using different methods. So, avoiding non-uniqueness of data explanation is the research focus on dust provenance.

Comparatively speaking, using detrital zircons to trace provenance is a more effective method. Zircon ($ZrSiO_4$) occurs in a wide variety of sedimentary, igneous, and metamorphic rocks. Zircon contains radioactive elements U and Th with long half lives. Due to the high U-Th-Pb closure temperature in zircon ($>900^\circ C$) [19], zircon is often used for dating. It is resistant to erosion, and the Earth's oldest known rocks were dated by zircons. Zircon can be determined U and Th, it also contains Hf and REE, which are good indicators of evolutionary processes of its host rock. Recently, the developments of in-situ microprobe techniques make it possible to study them on micrometer scale, and multistage geological events are revealed from a single zircon crystal, including various igneous and metamorphic processes caused by dissolution, modification, and newborn of zircons. Therefore, the source areas of zircon grains are constrained definitely by analyzing U-Pb ages and element composition of zircons. The relative contributions of different sources are estimated by multi-grain statistics. Compared with the potential desert sources, the processes before loess accumulation are now much better understood.

In this paper, we introduce the methods of detrital zircons to trace the provenance of loess, and take the Horqin sandy land and its surrounding loess as an example to semi-quantitatively estimate the sources.

1 The tracing methods of detrital zircons

Using detrital zircons to trace the provenance is to compare the zircon compositions of depositional area with those of potential source regions in order to determine the contribution of different sources to the sediments. These comparisons include internal structure, trace element, U-Pb age spectrum, and Hf isotopic compositions of detrital zircons.

1.1 Internal structure

The internal structure of zircon is often obtained by backscattered electron (BSE) imaging and cathodoluminescence (CL) imaging. BSE image reveals the difference of average molecule weight of zircon surface [20]. CL image shows the difference in the abundances of some trace ele-

ments (such as U, Y, Dy, Tb, etc.) and the defects in the crystal lattice of zircon. Generally, a negative correlation has been observed between the CL intensity and the trace element content of U, REE, Th, etc. [21, 22]. In most cases, The CL image reveals the most detailed internal structure of zircon.

Magmatic zircon usually has typical feature of well-developed magmatic oscillatory zoning. Sector zoning also occurred in magmatic zircon, which was formed in unstable environment that results in different growth velocities of crystal facies [23]. Some igneous zircons from mantle-derived rock show no or weakly zoned characteristic.

Metamorphic zircon has such internal structures as no zoning, weakly zoning, cloudy zoning, sector zoning, fir-tree zoning, planar zoning, patched zoning, spongy zoning, and flowed zoning [24].

1.2 Trace element compositions

A large number of investigations indicated that magmatic and metamorphic zircons can be distinguished by their Th and U contents and Th/U ratios. Magmatic zircons have higher Th and U contents as well as Th/U ratios (usually >0.4). Metamorphic zircons have lower Th and U contents as well as Th/U ratios (usually <0.1) [25]. However, if zircons crystallized from some melts that have peculiar chemical compositions, they would have anomalous Th/U ratios [26–28]. Other indices except Th/U ratios are needed to distinguish igneous and metamorphic zircons.

Trace element (especially REE) abundances in igneous zircons are used mostly to distinguish them from different rock types. Belousova et al. [28] analyzed concentrations of trace elements for zircons from a wide range of igneous rocks. They found that bi-variable discriminated diagrams and classic trees based on recursive techniques can provide a useful means of relating parent rock type to zircon trace element characteristics. There is a general trend of increasing trace element abundances in igneous zircons from ultramafic through mafic to granitic rocks. The average content of REE is less than 50 ppm in kimberlitic zircons, 600–700 ppm in lamproitic zircons, and about 2000 ppm in zircons from mafic rock, and can reach per cent levels in zircons from granitoid and pegmatite.

The trace element characteristics of metamorphic zircon can be used to relate their formation to metamorphic conditions. Metamorphic overgrowth of zircon in granulite-facies rocks generally has relative HREE depletion and obviously negative Eu anomaly [29, 30]. Metamorphic zircon formed under eclogite-facies conditions is usually depleted in HREE, and has low Nb and Ta contents and Nb/Ta ratio without significant Eu anomaly [25]. Amphibolite-facies zircon shows relatively HREE enrichment and clearly negative Eu anomaly [31].

1.3 U-Pb ages

At present, there are mainly three measurement techniques

of zircon U-Pb age. (1) TIMS (Thermal Ionization Mass Spectrometry): The zircons were decomposed by acids, U and Pb were extracted by anion exchange resin, and isotopic ratios of U and Pb were determined by isotope dilution method [32]. This method has high precision, but the sample treatment is complicated, requiring zircon decomposed and cannot implement *in situ* measurements. (2) SIMS (Secondary Ion Mass Spectrometry): This method need not dissolve zircons, and can obtain *in situ* results with high-spatial resolution to determine age of fine part of single zircon crystal [33] (the beam spot size is generally 20–50 μm , and even reduced to 5–8 μm). However, this method is time-consuming (about 20 min for every test spot) and with a high cost. Measurements of large numbers of zircon grains using above two methods are not suitable. (3) LA-ICP-MS (Inductively Coupled Plasma Mass Spectrometry): This method can realize *in situ* dating by laser ablation sampling [34]. In some condition, it can achieve the accuracy and precision comparable to SIMS, has a shorter analysis time (<4 min for every test spot), and is less expensive. It is an ideal analysis method for detrital zircons at present. Compared with SIMS, this method has some disadvantages such as larger sampling amount and more damage to samples (the spot size is generally 30–60 μm , and sampling depth is 10–20 μm). Although its spatial resolution and analysis precision were lower than SIMS, it can meet the requirement of detrital zircon analysis of loess.

There are two strategies in detrital zircon analysis. One approach is that grains from all color and morphology groups were analyzed irrespective of their abundance among the available grains [35]. This method has an advantage of including all possible age components when analysis of detrital zircon grains is small. Most TIMS and SIMS detrital zircon analyses follow this strategy. This strategy cannot reflect the relative contributions of different source components. Another approach is that at least 117 grains were measured randomly and proportions of different age components are calculated to estimate the contributions of potential sources statistically [36]. This strategy is widely applied with the development of LA-ICP-MS technique.

U-Pb age data are generally displayed using concordia diagrams to convey information about grain numbers of every sample analyzed, precision and concordance of every spot. However, as sample size increases, these concordia diagrams can become visually crowded. Thus concordant detrital zircon ages are commonly displayed in histograms and probability density distributions. Through comparison of detrital zircon age spectra of sediments with those of potential sources, the provenances can be constrained specifically, and then transport pathways be proposed. There are two mathematical methods to compare age spectra of detrital zircons commonly. One is that Sambridge et al. [37] developed a deconvolving method based on maximum likelihood algorithm in order to estimate the most likely ages, proportions, and number of components in a set of U-Pb age

spectra of detrital zircons. The other is the two-sample Kolmogorov-Smirnov (K-S) test that can provide a statistical basis for comparing the similarity of detrital zircon age spectra of sediments with those of potential sources [38].

1.4 Hf isotopic compositions

The geochemistry of Hf is virtually identical to Zr. Hence Hf is as a minor substitute for Zr in zircon (0.5%–2% Hf contained in zircon) [39]. Variations in the abundance of ^{176}Hf are conventionally expressed with respect to ^{177}Hf , which is stable nuclide. The β -decay of ^{176}Lu , which has a half-life of 37 Ga, produces ^{176}Hf . The content of Lu in zircon is very low. ^{176}Hf decayed from ^{176}Lu is very few. So, $^{176}\text{Hf}/^{177}\text{Hf}$ ratio of zircon effectively preserves the initial $^{176}\text{Hf}/^{177}\text{Hf}$ ratio at the time of zircon formation, and provides important information for genesis of the parent magma [40]. This combination of U-Pb ages and Hf isotopic compositions of single-grain detrital zircons makes it possible to determine, through each grain, not only the age but the nature and source of the host magma.

There are mainly two parameters to be considered to explain the source of zircon host magma by Hf isotopic ratio. One is $\varepsilon_{\text{Hf}}(t)$, which is the relative deviation in parts in 10^4 from the $^{176}\text{Hf}/^{177}\text{Hf}$ ratio of the chondritic uniform reservoir (CHUR) when the rock is formed.

$$\varepsilon_{\text{Hf}}(t) = 10000 \times \left\{ \frac{[(^{176}\text{Hf}/^{177}\text{Hf})_{\text{S}} - (^{176}\text{Lu}/^{177}\text{Hf})_{\text{S}} \times e^{\lambda t} - 1]}{[(^{176}\text{Hf}/^{177}\text{Hf})_{\text{CHUR},0} - (^{176}\text{Lu}/^{177}\text{Hf})_{\text{CHUR}} \times (e^{\lambda t} - 1)] - 1} \right\}$$

The initial Lu/Hf ratio of the Earth is approximately similar to that of the chondrite. The Lu/Hf ratio changed gradually as the upper mantle partially melted. During the course of producing basaltic magma, residual mantle is depleted in Hf (Hf is more incompatible than Lu), and basaltic crust is enriched in Hf correspondingly. As the time elapsed, the Hf isotope ratios of the depleted mantle (Lu/Hf > chondrite) and the enriched crust (Lu/Hf < chondrite) are different from those of non-differential primitive Earth (Lu/Hf = chondrite). When $\varepsilon_{\text{Hf}}(t) > 0$, it means that the rock comes from the depleted mantle (DM), and when $\varepsilon_{\text{Hf}}(t) < 0$, the rock comes from the enriched mantle (EM) or sources assimilated and contaminated by the Crust.

The other parameter is Hf model age relative to the depleted mantle (T_{DM}), including one and two-stage model age. In most cases, a two-stage model age should be considered for zircon [41], which signifies the age that the host magma of zircon comes from the mantle, i.e. crustal residence time.

$$T_{\text{DM}}^{\text{C}} = 1/\lambda \times \ln \left\{ 1 + \frac{[(^{176}\text{Hf}/^{177}\text{Hf})_{\text{S},t} - (^{176}\text{Hf}/^{177}\text{Hf})_{\text{DM},t}]}{[(^{176}\text{Lu}/^{177}\text{Hf})_{\text{C}} - (^{176}\text{Lu}/^{177}\text{Hf})_{\text{DM}}]} \right\} + t$$

When $\varepsilon_{\text{Hf}}(t)$ of zircon is positive and Hf model age is close to crystallization age, it shows that the source rock originates from newborn mantle material. Otherwise, it comes from remelting of the old crust [40].

Several above-mentioned characteristics of zircon combined are very effective to trace the provenance. For example, the composition of the Triassic Songpan-Ganzi complex is complicated. It is difficult to determine its sources using traditional methods. Weislogel et al. [38] compared the U-Pb zircon age spectra of this complex with those of surrounding potential sources systematically, and found that there are three kinds of compositions in the U-Pb zircon age spectra, correspond to three depocenters that sourced from different tectonic units respectively. Their work well constrained the provenance of this complex.

Although detrital zircon analysis is a powerful tool, the complexity of natural processes and the discrepancy of statistical methods of detrital zircon will affect the results of provenance explanation. The complexity begins with the source rocks themselves; for instance, zircon does not occur in all rocks (there are few zircons in ultramafic and mafic igneous rocks). Even if zircon is present, the rock type will determine the amount of zircon present, and then will overestimate or underestimate the contributions of some sources.

2 Applications of detrital zircons in the provenance of loess from Northeast China

The Horqin sandy land is located in the southwestern part of the Songliao Basin covering an area of 42300 km² with annual precipitation between 300–450 mm. There, most of the sand dunes are semi-stabilized [42]. There are loess deposits in the south and east of the Horqin sandy land. This region is distributed in the marginal zone of east Asian monsoon, which is very sensitive to monsoonal change. The geological records indicate that sand dunes in this region are active during the Last Glacial Maximum (LGM) and are stabilized during the Holocene Optimum (HO) [43]. Human activity and climate change in recent several thousand years make the trend worse [43]. So far, study on loess in this region is concentrated on luminescence dating and paleoclimatic reconstruction [44–46], with little concerns on loess provenance. Whether the surrounding loess comes from the Horqin sandy land? And where does the Horqin sandy land source from? These questions remain unanswered. We sampled the sands from the Horqin sandy land and loess from its surrounding loess deposit systematically, analyzed U-Pb ages and Hf isotopic compositions of detrital zircons, and compared them with those of neighboring tectonic units to determine the provenance of the loess and sandy land.

2.1 Geological setting and sampling

The Horqin sandy land and its surrounding loess are situated between the NCC to the south and the CAOB to the north (Figure 1(a)). The CAOB is a huge structural collage belt between the Siberia Craton and NCC. It formed mainly

from the progressive subduction and accretion of terranes of different types containing Precambrian microcontinental blocks, island arcs, accretionary complexes, ophiolites, and passive continental margins [47]. It is distributed by huge volumes of Paleozoic and Mesozoic intrusive and volcanic rocks. The northeastern part of the NCC consists of early Archean to Paleoproterozoic basement rocks overlain by unmetamorphosed Mesoproterozoic to Neoproterozoic volcanic-sedimentary sequences and Phanerozoic cover succession. The Phanerozoic strata are composed of the Cambrian-Middle Ordovician deposits dominated by neritic carbonates and a Late Carboniferous to Early Permian alternating marine and terrestrial sequence is characterized by carbonates and coal-bearing rocks, overlain by the Late Permian-Triassic red beds and conglomerates, and the Early Jurassic to the Early Cretaceous terrestrial volcanic and clastic sediments.

We sampled two typical sections of the Horqin sandy land deposited from the Last Glacial—KZH (42.70°N, 121.97°E) and SL (43.51°N, 123.38°E), and two loess sections—YC (42.12°N, 119.85°E) and SLB (41.87°N, 119.39°E) (Figure 1). These sand sections consist of yellow sand unit, whose lower part is not outcropped, and black sandy loam soil from the bottom up. The luminescence results indicate that the ages of boundary between yellow and black sand unit are from late Last Glacial to early Holocene, implying that yellow sand unit was deposited mainly during the Last Glacial and black sandy loam soil during the Holocene [50]. The loess sections are composed of the Last Glacial (L1) loess and the Holocene (S0) paleosol (Figure 2), which can be distinguished easily in field observation and magnetic susceptibility curve. We collected one sample from every sand and loess layer of the Last Glacial (Figure 2).

2.2 Experimental methods

About 1 kg samples were processed by elutriation, electromagnetic separation, and heavy liquid. Zircon grains with free inclusion and least fracture were handpicked and mounted on adhesive tape, enclosed in epoxy resin and then polished to expose zircon surface, and photographed in reflected and transmitted light. The mounts were then imaged under CL using a CAMECA SX51 scanning electron microscope at the Institute of Geology and Geophysics, Chinese Academy of Sciences. U-Pb age analyses were carried out on a Perkin-Elmer Sciex Elan6100DRC ICP-MS equipped with a 193 nm GeoLas200M laser, housed at State Key Laboratory of Continental Dynamics, the Department of Geology, Northwest University. In our analysis, zircon standard 91500 was used as an external calibration. The laser spot diameter was 30 μm. The detailed analytical procedures and parameters were described by Yuan et al. [51]. Common Pb was corrected according to the method proposed by Andersen [52]. Isotopic ratios and element con-

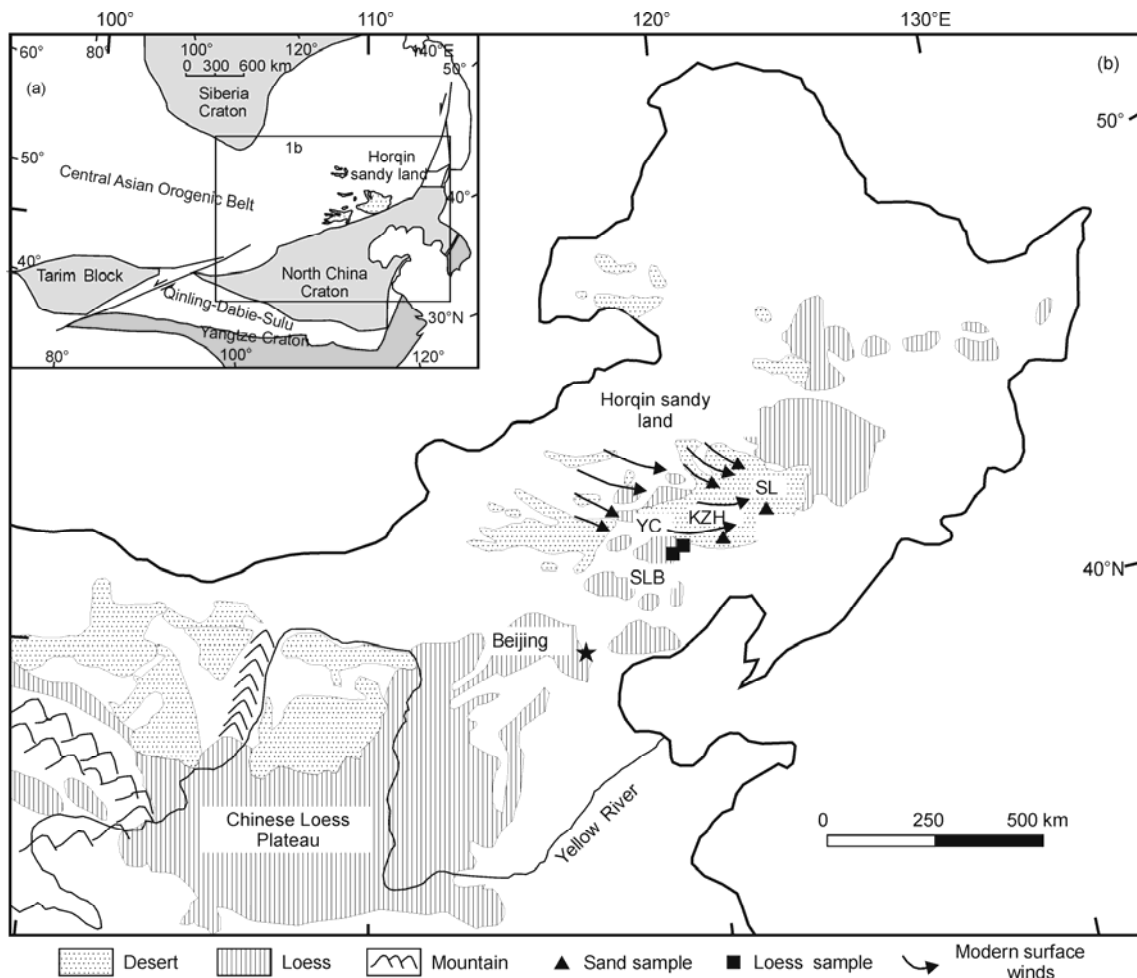


Figure 1 (a) Tectonic background map of the study area (modified from [48]); (b) map showing the profile location of the Horqin sandy land and its surrounding loess (based on ref. [49]).

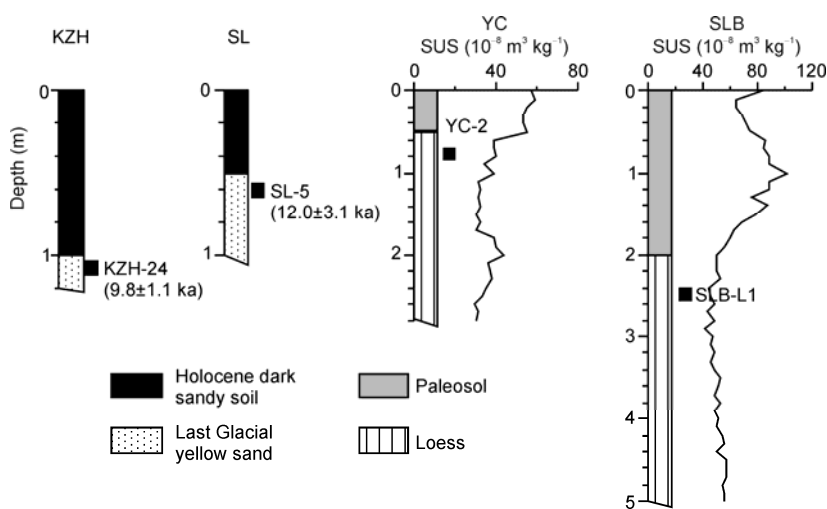


Figure 2 Stratigraphic map of the Horqin sandy land and its surrounding loess. The optical stimulated luminescence(OSL) ages are marked in bracket [50]. ■ Sampling position of detrital zircon.

centrations were calculated using the Glitter program (ver. 4.0). The age calculations and plotting of age spectra were made using Isoplot program (ver 3.0) [53]. We analyzed 120 grains of zircon from each sample arbitrarily. The $^{206}\text{Pb}/^{238}\text{U}$ ages were used for grains with $^{207}\text{Pb}/^{206}\text{Pb}$ ages <1000 Ma, and $^{207}\text{Pb}/^{206}\text{Pb}$ ages for older grains. Grains that are discordant by more than 10% were discarded.

Zircon Hf isotopic analyses were conducted using the Neptune MC-ICPMS at the Institute of Geology and Geophysics, Chinese Academy of Sciences. The spot size of 63 μm was used. During analyses, standard zircon 91500 was used for external correction. The operation condition of the instrument and detailed analytical technique is described in Xu et al. [54] The detailed procedures of data correction were described by Wu et al. [55].

2.3 Results

The lengths of zircons from sand sample KZH-24 and SL-5 are from 50 to 330 μm , and those from loess sample YC-2 and SLB-L1 are from 40 to 150 μm . Zircons from sand and loess samples are from euhedral prismatic and acicular to subhedral stubby and anhedral elliptical and rounded in morphology. Zircon colors include colorless, light yellow, light pink, and dark brown. There are all kinds of internal structure zircons in CL images. (1) Igneous zircon such as typical oscillatory zoning (Figure 3(a)), sector zoning (Fig-

ure 3(b)), and inherited core with oscillatory zoning overgrowth (Figure 3(c)). (2) Long prismatic or acicular zircon may be sourced from volcanic rocks. (3) Metamorphic zircon including overgrowth (Figure 3(e)), newborn such as no zoning (Figure 3(f)), weakly zoning (Figure 3(g)), and first zoning (Figure 3(h)), recrystallization (Figure 3(i)).

Th/U ratios of detrital zircons are mostly larger than 0.4, and only a few are smaller than 0.1. So, detrital zircons of the samples are sourced mainly from igneous rocks, and metamorphic zircons are rare.

The U-Pb detrital zircon spectra of sand samples from the Horqin sandy land can be divided mainly into three groups 2600–2300 Ma (peaks in 2500–2400 Ma), 2100–1600 Ma (peaks in 1800–1700 Ma), and 600–100 Ma. Therein, there are dense peaks in 600–100 Ma, and the peak of ca. 250 Ma is dominated. Loess samples are similar to the sand samples, and also consisted of these three groups (Figure 4).

The Hf isotopic compositions of loess detrital zircons are also identical to those of the Horqin sandy land (Figure 4). The detrital zircons can be divided into four groups according to U-Pb age and Hf isotope (Figure 5). The 2600–2100 Ma zircons have $\varepsilon_{\text{Hf}}(t)$ values of -9.3 – 8.7 mostly positive. The 2000–1500 Ma zircons have negative $\varepsilon_{\text{Hf}}(t)$ values of -10.1 – 6.8 . Phanerozoic zircons (546–121 Ma) can be classified into two groups according to $\varepsilon_{\text{Hf}}(t)$ values. Some zircons have negative $\varepsilon_{\text{Hf}}(t)$ values of -21 – 0.8 . The others

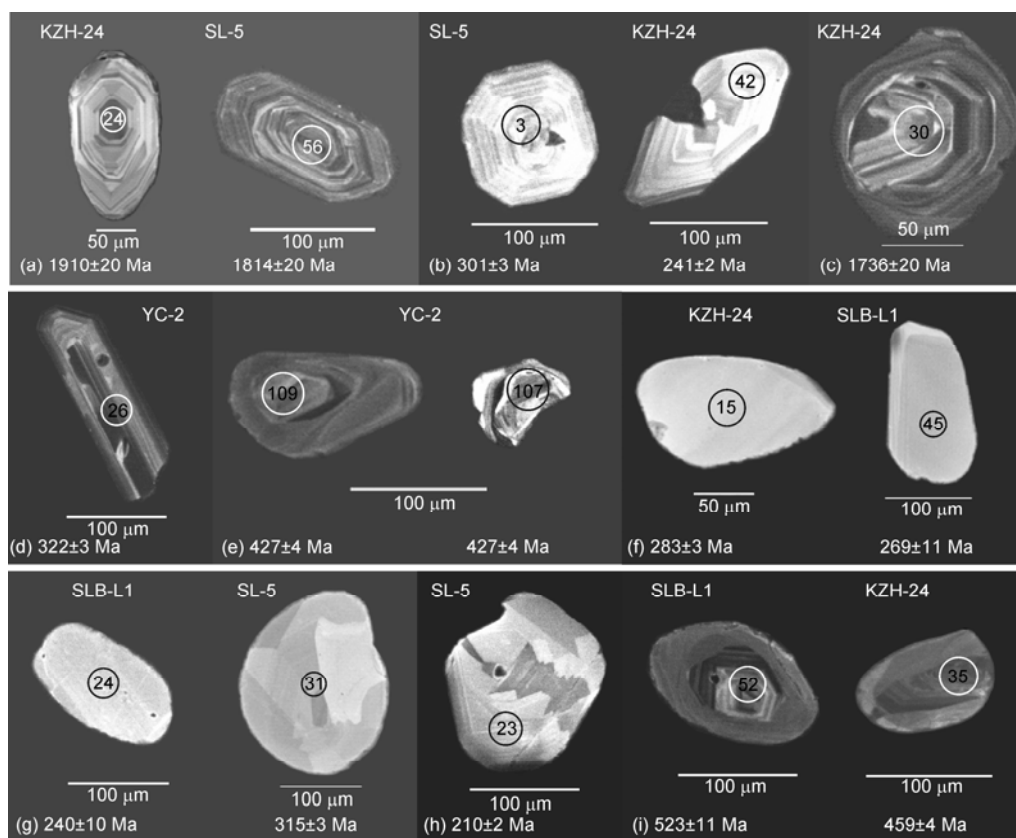


Figure 3 Representative cathodoluminescence (CL) images of detrital zircons from the Horqin sandy land and its surrounding loess.

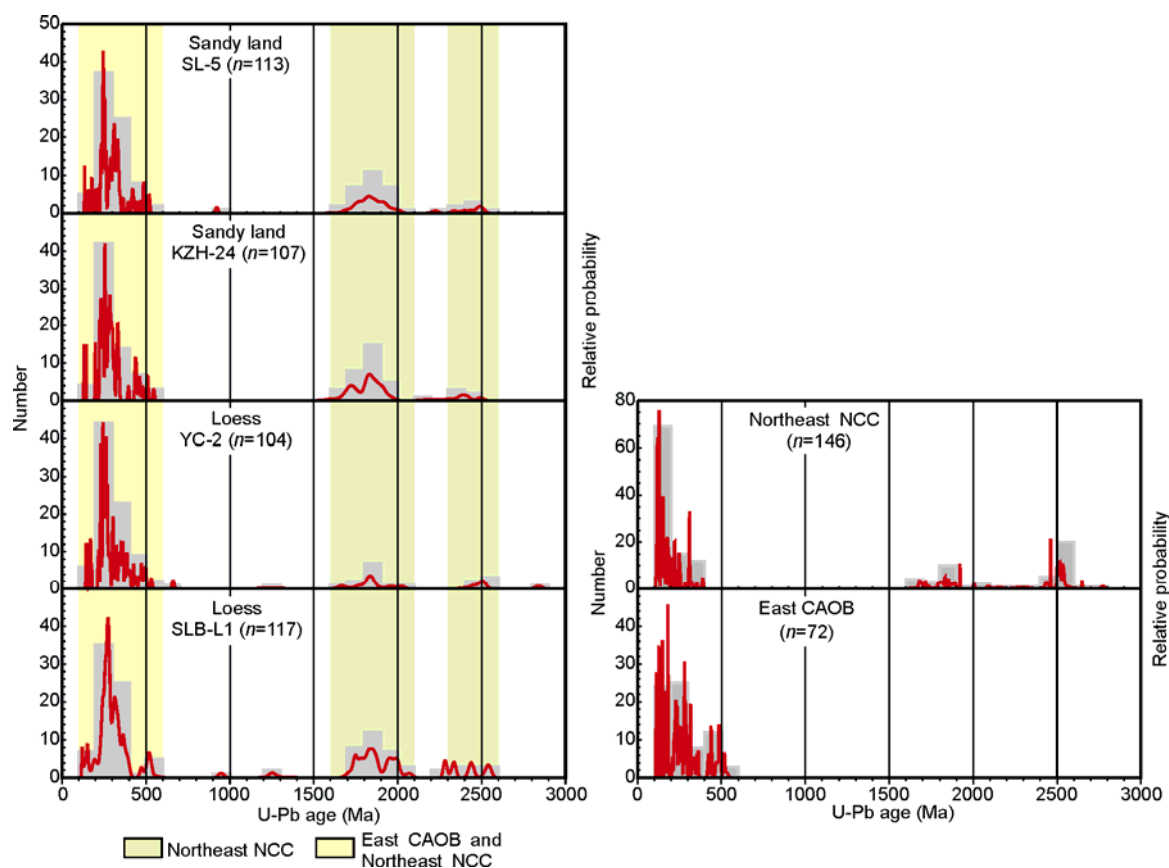


Figure 4 U-Pb age spectra of detrital zircons from the Horqin sandy land and south loess, and published U-Pb ages of igneous rocks from potential sources-Northeast NCC and East CAOB (data are from ref. [56] and references therein).

have positive $\varepsilon_{\text{Hf}}(t)$ values of -1.7 – 16.0 .

2.4 Discussion and conclusions

The U-Pb detrital zircon age spectra and Hf isotope of loess samples are similar to those of the Horqin sandy land, implying that the loess is sourced mainly from the Horqin sandy land during the Last Glacial period.

Igneous zircon ages from the eastern CAOB range broadly from 531 to 111 Ma, almost without Archean or Proterozoic ages (Figure 4) according to Yang et al. [56]. Paleozoic and Mesozoic garnites and volcanic rocks in the eastern CAOB have positive $\varepsilon_{\text{Nd}}(t)$ values, indicating that large amounts of juvenile mantle materials were added to the CAOB crust during the Phanerozoic [57]. Correspondingly, $\varepsilon_{\text{Hf}}(t)$ values of igneous rocks also have positive values [58]. Igneous zircons in the eastern CAOB have $\varepsilon_{\text{Hf}}(t)$ values ranging from -4.2 to 16.3 , with peaks at about 6.0 and 10.0 [56] (Figure 5). U-Pb ages of igneous zircons from northeastern NCC have age distribution peaks centered on 2600–2400, 1900–1700, and 390–111 Ma (Figure 4). Its Phanerozoic zircons have negative $\varepsilon_{\text{Hf}}(t)$ values of -3.8 – -22.8 , which is very different from Phanerozoic zircons of eastern CAOB (Figure 5).

In detrital zircons of loess and the Horqin sandy land, the

older Archean and Paleoproterozoic age group (2800–2100 Ma) have positive $\varepsilon_{\text{Hf}}(t)$ values, and the Paleoproterozoic age group (2000–1500 Ma) have negative $\varepsilon_{\text{Hf}}(t)$ values. The two groups are similar to the basement rocks of northeastern NCC, implying they may come from northeastern NCC. Phanerozoic zircons (546–121 Ma) can be divided into two groups according to their $\varepsilon_{\text{Hf}}(t)$ values. Zircons with positive $\varepsilon_{\text{Hf}}(t)$ values may come from eastern CAOB, and some with negative $\varepsilon_{\text{Hf}}(t)$ values may come from northeastern NCC. Few Meso- and Neoproterozoic zircons occur in some samples, whose $\varepsilon_{\text{Hf}}(t)$ values change broadly. They may originate from several sources. Therein, zircon ages of ca. 900 Ma may be consistent with Neoproterozoic magmatic activity of northern NCC [59].

We count detrital zircon grains derived from northeastern NCC and eastern CAOB, and calculate percentages of different sources to estimate the contributions. The northeastern NCC may contribute 49%–61% to the Horqin sandy land and its surrounding loess (54% on average), and the eastern CAOB is about 46%. Materials derived from the northeastern NCC and eastern CAOB may be transported by fluvial system and wind to the Horqin sandy land, and then transported to downwind loess deposit area by wind. Detrital zircon characteristics of the Horqin sandy land and its surrounding loess are clearly different from the Chinese

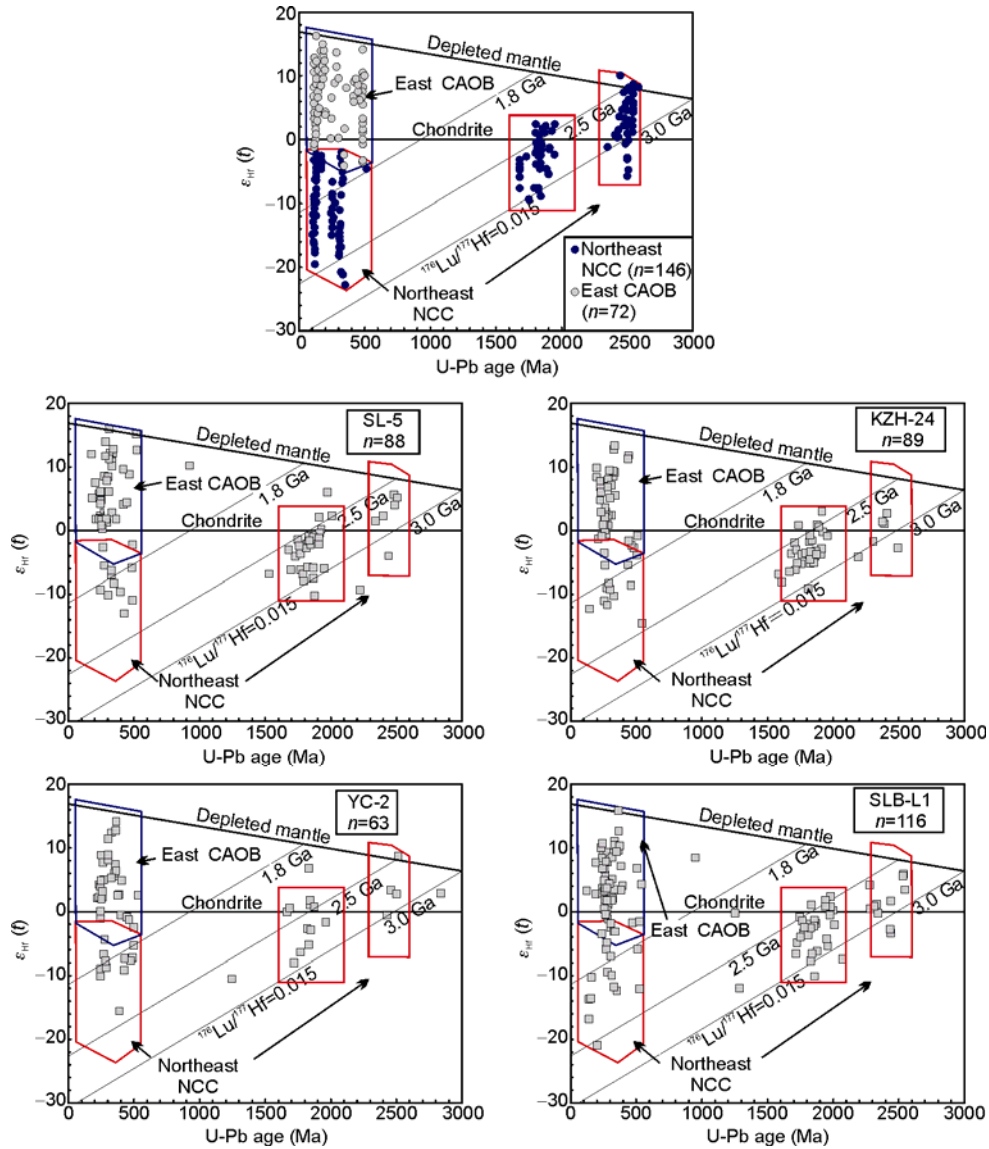


Figure 5 Diagram of $\epsilon_{\text{Hf}}(t)$ vs. U-Pb ages from the Horqin sandy land and its south loess, and published data from potential sources—Northeast NCC and East CAOB (data are from ref. [56] and references therein).

Loess Plateau and central-western deserts [60]. The U-Pb detrital zircon age spectra of the Loess Plateau are distributed in early Paleozoic of 243–382 Ma with peaks at ca. 280 Ma, late Paleozoic of 400–540 Ma, Meso- and Neoproterozoic age peaks in 590, 656, 800–1100, 1200–1500 Ma, and a few in Paleoproterozoic of 1600–1900 Ma and late Archean, without any young Mesozoic grains. The Horqin sandy land and proximal loess have much fewer late Paleozoic zircons than the Loess Plateau, almost absent of Meso- and Neoproterozoic age, and have Mesozoic grains of 100–200 Ma. So, loess surrounding of the Horqin sandy land is a kind of short-range transportation deposit entrained by the near-surface winds.

From this application instance, it is evident that detrital zircon is an effective method of tracing loess provenance, and it determines not only which desert it comes from, but

also which crystalline rocks it comes from by comparison with proximal tectonic unit. This method can establish the connection that material eroded from crystalline rocks deposits to loess accumulation area passing by the deserts. Certainly, limited by instrument techniques and zircon grain picking, the zircon grain size analyzed is coarse in most laboratories. Recently, study on dating fine grain zircon is developed in some laboratories, and some data have been published [61, 62]. As the techniques improving, measurements of fine size zircons will be popularized gradually. So, using detrital zircons to trace the provenance of loess will have a very wide application prospect.

We thank Prof. Liu Xiaoming, Yuan Honglin, Xie Liewen, and Yang Yueheng for their assistance with experiment analyses. Dr. Yang Lirong provided OSL age data of the sandy land samples. Dr. Tang Zihua and

Wang Xu improved the manuscript. This work was supported by Young Scholars of the National Natural Science Foundation of China (Grant No. 40802037), National Basic Research Program of China (Grant No. 2010CB950204) and Knowledge Innovation Program of the Chinese Academy of Sciences (Grant No. 80972970). The U-Pb age and Hf isotope data in this article can be obtained by sending email to the authors.

- 1 Guan Q Y, Pan B T, Gao H S, et al. Geochemical evidence of the Chinese loess provenance during the Late Pleistocene. *Paleogeogr Paleoclimatol Paleoecol*, 2008, 270: 53–58
- 2 Ferrat M, Weiss D J, Strekopytov S, et al. Improved provenance tracing of Asian dust sources using rare earth elements and selected trace elements for palaeomonsoon studies on the eastern Tibetan Plateau. *Geochim Cosmochim Acta*, 2011, 75: 6374–6399
- 3 Chen J, Li G J. Geochemical studies on the source region of Asian dust. *Sci China Ser D-Earth Sci*, 2011, 54: 1279–1301
- 4 Chen J, Li G J, Yang J D, et al. Nd and Sr isotopic characteristics of Chinese deserts: Implications for the provenances of Asian dust. *Geochim Cosmochim Acta*, 2007, 71: 3904–3914
- 5 Li F. Distribution characteristics of lead isotope in dust source areas and its trace significance in the North of China (in Chinese). *J Desert Res*, 2007, 27: 738–744
- 6 Pettke T, Lee D, Halliday A N, et al. Radiogenic Hf isotopic compositions of continental eolian dust from Asia, its variability and its implications for seawater Hf. *Earth Planet Sci Lett*, 2002, 202: 453–464
- 7 Hattori Y, Suzuki K, Honda M, et al. Re-Os isotope systematics of the Taklimakan Desert sands, moraines and river sediments around the Taklimakan Desert, and of Tibetan soils. *Geochim Cosmochim Acta*, 2003, 67: 1195–1205
- 8 Aleon J, Chaussidon M, Marty B, et al. Oxygen isotopes in single micrometer-sized quartz grains: tracing the source of Saharan dust over long-distance atmospheric transport. *Geochim Cosmochim Acta*, 2002, 66: 3351–3365
- 9 Sun Y B, Tada R, Chen J, et al. Distinguishing the sources of Asian dust based on electron spin resonance signal intensity and crystallinity of quartz. *Atmos Environ*, 2007, 41: 8537–8548
- 10 Li G J, Chen J, Chen Y, et al. Dolomite as a tracer for the source regions of Asian dust. *J Geophys Res*, 2007, 112: D17201
- 11 Derbyshire E, Meng X M, Kemp R A. Provenance, transport and characteristics of modern eolian dust in western Gansu Province, China, and interpretation of the Quaternary loess record. *J Arid Environ*, 1998, 39: 497–516
- 12 Lu H Y, Sun D H. Pathways of dust input to the Chinese Loess Plateau during the last glacial and interglacial periods. *Catena*, 2000, 40: 251–261
- 13 Muhs D R, Bettis E A. Geochemical variations in Peoria Loess of Western Iowa indicate paleowinds of midcontinental North America during Last Glaciation. *Quat Res*, 2000, 53: 49–61
- 14 Yang S, Ding Z. Advance-retreat history of the East-Asian summer monsoon rainfall belt over northern China during the last two glacial-interglacial cycles. *Earth Planet Sci Lett*, 2008, 274: 499–510
- 15 Liu T S. *Loess and Environment*. Beijing: China Ocean Press, 1985. 1–321
- 16 Ding Z L, Sun J M, Yang S L, et al. Geochemistry of the Pliocene red clay formation in the Chinese Loess Plateau and implications for its origin, source provenance and paleoclimate change. *Geochim Cosmochim Acta*, 2001, 65: 901–913
- 17 Gallet S, Jahn B M, Morii M. Geochemical characterization of the Luoquan loess-paleosol sequence, China, and paleoclimatic implications. *Chem Geol*, 1996, 133: 67–88
- 18 Jahn B M, Gallet S, Han J M. Geochemistry of the Xining, Xifeng and Jixian sections, Loess Plateau of China: Eolian dust provenance and paleo sol evolution during the last 140 ka. *Chem Geol*, 2001, 178: 71–94
- 19 Moller A, O'Brien P J, Kennedy A, et al. Polyphase zircon in ultra-high-temperature granulites (Rogaland, SW Norway): Constraints for Pb diffusion in zircon. *J Metamorph Geol*, 2002, 20: 727–740
- 20 Hanchar J M, Miller C F. Zircon zonation patterns as revealed by cathodoluminescence and backscattered electron images: Implications for interpretation of complex crustal histories. *Chem Geol*, 1993, 110: 1–13
- 21 Crofu F, Hanchar J M, Hoskin P W O, et al. Atlas of zircon textures. *Rev Mineral Geochem*, 2003, 53: 469–495
- 22 Rubatto D, Gebauer D. Use of cathodoluminescence for U-Pb zircon dating by IOM Microprobe: Some examples from the western Alps. In: Pagel M, Barbin V, Blanc P, et al, eds. *Cathodoluminescence in Geoscience*. Berlin: Springer-Verlag, 2000. 373–400
- 23 Vavra G, Gebauer D, Schmid R. Multiple zircon growth and recrystallization during polyphase Late Carboniferous to Triassic metamorphism in granulites of the Ivrea Zone (Southern Alps): An ion microprobe (SHRIMP) study. *Contrib Mineral Petrol*, 1996, 122: 337–358
- 24 Wu Y B, Zheng Y F. Genesis of zircon and its constraints on interpretation of U-Pb age. *Chin Sci Bull*, 2004, 49: 1554–1569
- 25 Rubatto D. Zircon trace element geochemistry: Partitioning with garnet and link between U-Pb ages and metamorphism. *Chem Geol*, 2002, 184: 123–138
- 26 Wu Y B, Chen D G, Xia Q K, et al. *In-situ* trace element analyses of zircons from Dabieshan Huangzhen eclogite: Trace-element characteristics of eclogite-facies metamorphic zircon. *Chin Sci Bull*, 2002, 47: 1398–1401
- 27 Hidaka H, Shimizu H, Adachi M. U-Pb geochronology and REE geochemistry of zircons from Palaeoproterozoic paragneiss clasts in the Mesozoic Kamiaso conglomerate, central Japan: Evidence for an Archean provenance. *Chem Geol*, 2002, 187: 278–293
- 28 Belousova E A, Griffin W L, O'Reilly S Y, et al. Igneous zircon: Trace element composition as an indicator of source rock type. *Contrib Mineral Petrol*, 2002, 143: 602–622
- 29 Whitehouse M J, Platt J P. Dating high-grade metamorphism constraints from rare-earth elements in zircons and garnet. *Contrib Mineral Petrol*, 2003, 145: 61–74
- 30 Wu Y B, Chen D G, Xia Q K, et al. *In-situ* trace element analyses and Pb-Pb dating of zircons in granulite from Huangtuling, Dabieshan by LAM-ICP-MS. *Sci China Ser D-Earth Sci*, 2003, 46: 1161–1170
- 31 Hermann J, Rubatto D, Korsakov A. Multiple zircon growth during fast exhumation of diamondiferous, deeply subducted continental crust (Kokchetav Massif, Kazakhstan). *Contrib Mineral Petrol*, 2001, 141: 66–82
- 32 Krogh T E. A low contamination method for hydrothermal decomposition of zircon and extraction of U and Pb for isotopic age determinations. *Geochim Cosmochim Acta*, 1973, 37: 485–494
- 33 Ireland T R, Williams I S. Considerations in zircon geochronology by SIMS. *Rev Mineral Geochem*, 2003, 53: 215–241
- 34 Kosler J, Sylvester P J. Present trends and future of zircon in geochronology: Laser ablation ICPMS. *Rev Mineral Geochem*, 2003, 53: 243–275
- 35 Gehrels G E, Dickinson W R. Detrital zircon provenance of Cambrian to Triassic miogeoclinal and eugeoclinal strata in Nevada. *Am J Sci*, 1995, 295: 18–48
- 36 Vermeesch P. How many grains are needed for a provenance study? *Earth Planet Sci Lett*, 2004, 224: 441–451
- 37 Sambridge M S, Compston W. Mixture modeling of multi-component data sets with application to ion-probe zircon ages. *Earth Planet Sci Lett*, 1994, 128: 373–390
- 38 Weislogel A L, Graham S A, Chang E Z, et al. Detrital zircon provenance from three turbidite depocenters of the Middle-Upper Triassic Songpan-Ganzi complex, central China: Record of collisional tectonics, erosional exhumation, and sediment production. *Geol Soc Am Bull*, 2010, 122: 2041–2062
- 39 Hoskin P W O, Schaltegger U. The composition of zircon and igneous and metamorphic petrogenesis. *Rev Mineral Geochem*, 2003, 53: 27–55
- 40 Kinny P D, Maas R. Lu-Hf and Sm-Nd isotope systems in zircon. *Rev Mineral Geochem*, 2003, 53: 327–341
- 41 Wu F Y, Li X H, Zheng Y F, et al. Lu-Hf isotopic systematics and their applications in petrology (in Chinese). *Acta Petrol Sin*, 2007, 23: 185–220
- 42 Zhu Z D, Wu Z, Liu S, et al. An Outline on Chinese Deserts (in Chi-

- nese). Beijing: Science Press, 1980. 1–107
- 43 Sun J M, Ding Z L, Liu T S. Desert distributions during the glacial maximum and climatic optimum: Example of China. *Episodes*, 1998, 21: 28–31
- 44 Zhao H, Lu Y C, Yin J H. SAR dating of quartz and geochronology of Holocene sand dune activities in Horqin sandyfield, China (in Chinese). *Nuclear Techniques*, 2005, 28: 367–374
- 45 Qiu S W. Present situation, cause and comprehensive treatment of sandy desertification in western Northeast Plain, China (in Chinese). *J Desert Res*, 2004, 24: 124–128
- 46 Ge S W, Lu H Y, Zhou Y L, et al. The wet-dry variations of the Horqin sandy field by loess deposit of the late Quaternary (in Chinese). *J Desert Res*, 2006, 26: 869–874
- 47 Xiao W J, Windley B F, Hao J, et al. Accretion leading to collision and the Permian Solonker suture, Inner Mongolia, China: Termination of the central Asian orogenic belt. *Tectonics*, 2003, 22: 1069
- 48 Li J Y. Permian geodynamic setting of Northeast China and adjacent regions: Closure of the Paleo-Asian Ocean and subduction of the Paleo-Pacific Plate. *J Asian Earth Sci*, 2006, 26: 207–224
- 49 Sun J M. Provenance of loess material and formation of loess deposits on the Chinese Loess Plateau. *Earth Planet Sci Lett*, 2002, 203: 845–859
- 50 Yang L R. Distribution and environment of deserts of eastern China since LGM (in Chinese). Dissertation for the Doctoral Degree. Beijing: Graduate University of Chinese Academy of Sciences, 2007. 1–113
- 51 Yuan H L, Gao S, Liu X M, et al. Accurate U-Pb age and trace element determinations of zircon by Laser Ablation-Inductively Coupled Plasma-Mass Spectrometry. *Geostand Geoanal Res*, 2004, 28: 353–370
- 52 Andersen T. Correction of common Pb in U-Pb analyses that do not report ^{204}Pb . *Chem Geol*, 2002, 192: 59–79
- 53 Ludwig K R. User's Manual for Isoplot Version 3.0: A Geochronological toolkit for Microsoft Excel. Berkeley Geochronological Center, Special Publication, 2003. 4
- 54 Xu P, Wu F Y, Xie L W, et al. Hf isotopic compositions of the standard zircons for U-Pb dating. *Chin Sci Bull*, 2004, 49: 1642–1648
- 55 Wu F Y, Yang Y H, Xie L W, et al. Hf isotopic compositions of the standard zircons and baddeleyites used in U-Pb geochronology. *Chem Geol*, 2006, 234: 105–126
- 56 Yang J H, Wu F Y, Shao J A, et al. Constraints on the timing of uplift of the Yanshan Fold and Thrust Belt, North China. *Earth Planet Sci Lett*, 2006, 246: 336–352
- 57 Jahn B M, Wu F Y, Chen B. Massive granitoid generation in Central Asia: Nd isotope evidence and implication for continental growth in the Phanerozoic. *Episodes*, 2000, 23: 82–92
- 58 Xie J, Wu F Y, Ding Z L. Detrital zircon composition of U-Pb ages and Hf isotope of the Hunshandake sandland and implications for its provenance (in Chinese). *Acta Petrol Sin*, 2007, 23: 523–528
- 59 Peng P, Bleeker W, Ernst RE, et al. U-Pb baddeleyite ages, distribution and geochemistry of 925 Ma mafic dykes and 900 Ma sills in the North China Craton: Evidence for a Neoproterozoic mantle plume. *Lithos*, 2011, 127: 210–221
- 60 Steven T, Palk C, Carter A, et al. Assessing the provenance of loess and desert sediments in northern China using U-Pb dating and morphology of detrital zircons. *Geol Soc Am Bull*, 2010, 122: 1331–1344
- 61 Pullen A, Kapp P, McCallister A T, et al. Qaidam Basin and northern Tibetan Plateau as dust sources for the Chinese Loess Plateau and paleoclimatic implications. *Geology*, 2011, 39: 1031–1034
- 62 Liu Y, Li X H, Li Q L, et al. Precise U-Pb zircon dating at <5 micron scale by Cameca 1280 SIMS using Gaussian illumination probe. *J Anal At Spectrom*, 2011, 26: 845–851